POROSITY SENSOR

Vojko Matko

University of Maribor, Faculty of Electrical Engineering and Computer Science, Maribor, Slovenia

Key words: porosity, soils, glass test tube, capacitive-dependent crystal, direct digital method.

Abstract: In response to a need for a more accurate porosity measuring method for small solid samples (approximately 1 g in mass) the porosity measurement sensor using a sensitive capacitive-dependent crystal was developed. This paper presents the new sensor and the probe sensitivity, frequency dependence on the volume. In addition, the new idea of excitation of the entire sensor with stochastic test signals is described, and the porosity measuring method is provided. The latter includes the influence of test signals on the weighting function uncertainty. The experimental results of the porosity determination in volcanic rock samples are presented. The uncertainty of the porosity measurement is less than 0.1 % in the temperature range 10 - 30 °C.

Senzor poroznosti

Ključne besede: poroznost, zemljine, steklena merilna epruveta, kapacitivno odvisni kristali, direktna digitalna metoda.

Izvleček: V iskanju bolj natančnega merjenja poroznosti malih trdnih delcev (mase približno 1g) je bila razvita metoda, ki uporablja kapacitivno odvisne kristale. V delu je prikazan novi senzor in njegova frekvenčna odvisnost od volumna. V nadaljevanju je prikazana nova ideja vzbujanja senzorja s stohastičnimi signali in zmanjšanje merilne negotovosti vpliva sistema (senzorja). Prikazani so eksperimentalni rezultati merjenja poroznosti vulkanskega pepela s pogreškom 0.1% v temperaturnem območju 10 - 30°C.

1 Introduction

Porosity is defined as the ratio of the volume of voids to the total volume of the material.

Solid rock is often not so solid. Sandstone might have started out as a sand dune or a beach, which got buried and compressed. But spaces and pores, remain between the particles. Soils, too, contain pores, which can be classified as micro and macro. Pore diameters larger than 0.06 mm are called macropores and those less as micropores. Soils may be considered as a porous four-phase system composed of air, water, solids and admixtures. The latter are a mixture of water and solids and are soft. In this four-phase soil system, the density ρ of soils is defined as the ratio of the sum of mass m to the sum of volume V of various soil phases /1/-/3/

$$\rho = \frac{\sum m_i}{\sum V_i} = \frac{m_s + m_w + m_a + m_{ad}}{V_s + V_w + V_a + V_{ad}}, \quad (1)$$

$$\sum_i m_i = m_s + m_w + m_a + m_{ad}, \quad (2)$$

$$\sum_i V_i = V_s + V_w + V_a + V_{ad} \quad (3)$$

where

s	solid phase
w	water phase
a	air phase
ad	admixture.

Equation (1) can also be rewritten as

$$\rho = \frac{\rho_s V_s + \rho_w V_w + \rho_a V_a + \rho_{ad} V_{ad}}{V_s + V_w + V_a + V_{ad}}, \quad (4)$$

where solid particle density is

$$\rho_s = \frac{m_s}{V_s}, \quad (5)$$

water phase density is

$$\rho_w = \frac{m_w}{V_w}, \quad (6)$$

air phase density is

$$\rho_a = \frac{m_a}{V_a}, \quad (7)$$

and soil admixture density is

$$\rho_{ad} = \frac{m_{ad}}{V_{ad}}. \quad (8)$$

Instead of density, the specific gravity can be written. From equation (4) we can write

$$\gamma = \frac{(\rho_s V_s + \rho_w V_w + \rho_a V_a + \rho_{ad} V_{ad}) \cdot g}{V_s + V_w + V_a + V_{ad}}, \quad (9)$$

In practice, we can define mass as the ratio of weight of soil to gravity

$$m = \frac{W}{g}. \quad (10)$$

During weighting in air the mass must be increased due to the presence of the air (Avogadro's law)

$$m_s = \frac{W_s}{g} + \rho_a \cdot V_s, \quad (11)$$

$$m_w = \frac{W_w}{g} + \rho_a \cdot V_w, \quad (12)$$

$$m_{ad} = \frac{W_{ad}}{g} + \rho_a \cdot V_{ad}. \quad (13)$$

Porosity of soil is defined by two parameters - void ratio e and porosity parameter η. The total void ratio e is defined as the ratio of volume of pores to volume of solid particles

$$e = \frac{V_w + V_a}{V_s} \quad (14)$$

and phases void ratio as

$$e_w = \frac{V_w}{V_s}, \quad (15)$$

$$e_a = \frac{V_a}{V_s}. \quad (16)$$

The porosity parameter η is defined as the ratio of volume of water plus volume of air to volume of soil samples.

Total:

$$\eta = \frac{V_w + V_a}{V} = \frac{V_w + V_a}{V_s + V_w + V_a}. \quad (17)$$

Phases:

$$\eta_w = \frac{V_w}{V} = \frac{V_w}{V_s + V_w + V_a}, \quad (18)$$

$$\eta_a = \frac{V_a}{V} = \frac{V_a}{V_s + V_w + V_a}. \quad (19)$$

The water content w_a is defined as the ratio of the weight of water to the weight of soil particles

$$w = \frac{W_w}{W_s} = \frac{W - W_a - W_s - W_{ad}}{W_s}. \quad (20)$$

The absolute water content w_a is defined as the ratio of the weight of water to the total weight of sample

$$w_a = \frac{W_w}{W} = \frac{W - W_a - W_s - W_{ad}}{W}. \quad (21)$$

The degree of saturation S_r is defined as the ratio of the volume of pores saturated with water to the volume of all pores

$$S_r = \frac{V_w}{V_w + V_a} = \frac{\eta_w}{\eta_w + \eta_a}. \quad (22)$$

1.1 Porosity determination methods

The simplest method is the determination of porosity by saturation method (Fig. 1) /4/. In this standardised procedure, the beakers are first filled to the same mark with gravel, sand, silt or mixture of these three materials. Then the water is poured into each of the beakers until it reaches the top of each material.

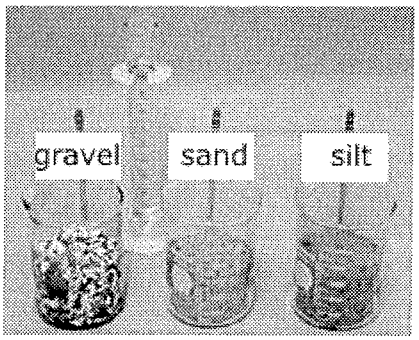

Fig. 1. Determination of porosity by saturation.

Porosity is determined by dividing the volume of water that you were able to pour into the material by the total volume of that material. The result is expressed as a percentage. It dictates how much water a saturated material can contain and has an important influence on bulk properties of material, e.g. bulk density, heat capacity, seismic velocity, etc.

$$\eta = \frac{V_{void}}{V_{total}} \cdot 100\ \% \quad (23)$$

where

V_{void} pore space volume

V_{total} total volume

There are many different porosity measurement methods. The imaging porosity method aims to identify and quantify different pore systems to determine the nature and abundance of matrix and macroporosity. Matrix porosity is characterised from digital images obtained from thin sections cut from core plugs /5/.

The helium pycnometer method uses helium. The pycnometer consists of two chambers, connected by a tube with a valve in it. The idea is to measure the pressure difference between the two containers, one of which has the sample material in it. The degree of porosity is determined by the difference in the pressures (due to porosity) caused by the opening of the valve at constant temperature. The porosity of the sample is the percentage difference between the grain volume and bulk volume, divided by the bulk volume /6/.

Porosity can also be determined by other conventional methods such as adsorption method, infrared scattering, mercury porosimetry, capillary method, dielectric method, analytical method, proton nuclear magnetic resonance, chromatography and ultrasound method /7/, /8/.

The new porosity measuring method described in this paper uses a highly sensitive sensor with improved uncertainty of measuring results and reduced influence of disturbing noise signals /9/. In comparison to the helium pycnometer method it is a lot simpler. In addition, the water is not poured on the material. Instead, the soil or rock sample is immersed in the water.

Most capacitive bridge methods can be adapted to three-terminal measurements by the addition of components to balance the ground admittances /10/, /11/. However, the balance conditions for these and the main bridge being interdependent, the balancing process can become very tedious. Also, the ratio signal/noise is supposed to be high.

The well-known method is Miller's etalon /12/ which is designed to sense small changes in the ≅ 4 pF capacitor from the phase change of a series-resonant circuit. The weakness of Miller's etalon is a greater sensitivity to phase noise than with the bridge method, which is due to higher frequencies (up to 45 MHz).

An alternative approach has been described by Van Degrift /13/ who used very sensitive tunnel-diode oscillator systems for measuring extremely small capacitance changes. This gain in sensitivity is somewhat offset by a loss in stability.

2 The porosity sensor

The porosity sensor uses sensitive capacitive-dependent crystals (40 MHz with stability of ±1 ppm in the temperature range from -5 to +55 °C) due to stability and the long-term repetition (Fig. 2). Two pseudo stochastic three-state signals $x_1(t)$ and $x_2(t)$ are used to influence the frequencies of the two quartz oscillators /14/, /15/. The frequency of oscillator 1 is 40 MHz and that of oscillator 2 is 40.001 MHz /16/, /17/. The output of the pulse-width modulator (EXOR) is a pulse-width signal which is compensated for temperature and voltage drift.

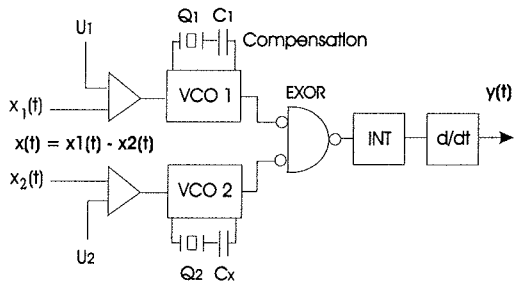

Fig. 2. Sensor structure.

The sensor probe C_x is a capacitor on the outer surface of the glass test tube (Fig. 3) /18/. The crystal is used as a stable oscillation element whose substitutional electrical structure only is being changed through the variation of the series capacitance C_x. The values in the quartz substitutional electrical structure and the capacitance C_x = 5 pF are measured with impedance/gain phase analyser HP 4194A.

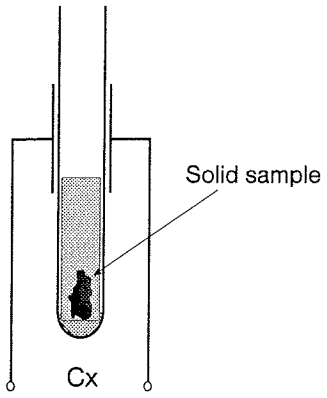

Fig. 3. Glass test tube.

The change of the water level causes the change of capacitance and frequency change in oscillator 2 (Fig. 2, Fig. 3). The probe dependence *df* on the volume is shown in Fig. 4. The frequency measurement uncertainty is ±0.1 Hz. The results suggest that the change in frequency is proportional to the volume in the range 0 - 1ml.

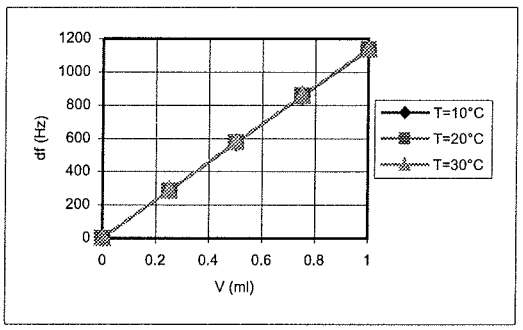

Fig. 4. The probe dependence df on the volume with signals $x_1(t)$ *and* $x_2(t)$.

3 Reduction of the measurement uncertainty

The uncertainty of the measuring results is improved by the direct digital method (DDM), which reduces the influence of disturbances /9/. Linear time-invariant system has been chosen due to signals $x_1(t)$ and $x_2(t)$, which form a special correlation function that is real-time independent.

$$\Phi_{xy}(\tau) = \sum_{u=0}^{T} g(u) \cdot \Phi_{xx}(\tau - u) \qquad (24)$$

$\Phi_{xy}(\tau)$ - cross-correlation function

$g(u)$ - weighting function

$\Phi_{xx}(\tau - u)$ - auto-correlation function

T - measuring period

For every value of τ, one equation with various numbers of elements is obtained. To calculate the value of the weighting functions g(0), g(1),..., g(L), the equations are united in the system with $L + 1$ equations

$$\begin{bmatrix} \Phi_{xy}(-P+L) \\ \cdot \\ \cdot \\ \Phi_{xy}(-1) \\ \Phi_{xy}(0) \\ \Phi_{xy}(+1) \\ \cdot \\ \cdot \\ \Phi_{xy}(M) \end{bmatrix} = \begin{bmatrix} \Phi_{xx}(-P+L) & \cdots & \Phi_{xx}(-P) \\ \cdot & \cdots & \\ \cdot & \cdots & \\ \Phi_{xx}(-1) & \cdots & \Phi_{xx}(-1-L) \\ \Phi_{xx}(0) & & \Phi_{xx}(-L) \\ \Phi_{xx}(+1) & & \Phi_{xx}(1-L) \\ \cdot & \cdots & \\ \cdot & & \\ \Phi_{xx}(M) & & \Phi_{xx}(M-L) \end{bmatrix} \cdot \begin{bmatrix} g(0) \\ \cdot \\ \cdot \\ \cdot \\ \cdot \\ \cdot \\ \cdot \\ \cdot \\ g(L) \end{bmatrix}$$

or its mathematical equivalent

$$\underline{\hat{\Phi}_{xy}} = \underline{\hat{\Phi}_{xx}} \cdot \underline{g}. \tag{25}$$

The biggest negative time move $\tau_{min} = -P$ and the biggest positive one $\tau_{max} = M$ were used. The system of equations has thus $P - L + M + 1$ number of equations. If $M = -P + 2L$ is chosen, $L + 1$ number of equations remain, so that $\hat{\Phi}_{xx}$ becomes a square matrix and we get

$$\hat{g} = \hat{\Phi}_{xx}^{-1} \cdot \hat{\Phi}_{xy}. \tag{26}$$

If $P = L$ is determined, then the same number of values (symmetrical auto-correlation functions (AKF) because $\tau_{min} = -P = -L$ and $\tau_{max} = M = L$ for the positive and negative τ) is used to calculate $\Phi_{xx}(\tau)$. The calculation of the weighting function is simplified if the input signal is white noise with the auto-correlation function as

$$\Phi_{xx}(\tau) = \sigma_x^2 \cdot \delta(\tau) = \Phi_{xx}(0) \cdot \delta(\tau), \tag{27}$$

$$\delta(\tau) \begin{cases} 1 \ for \ \tau = 0 \\ 0 \ for \ |\tau| \neq 0 \end{cases}. \tag{28}$$

It follows that

$$\hat{g}(\tau) = \frac{1}{\hat{\Phi}_{xx}(0)} \cdot \hat{\Phi}_{xy}(\tau). \tag{29}$$

Having formulated (26) and having considered the measurement time t_{meas} which is to be as long as possible, we get the weighting function $\hat{g}(\tau)$ (29) /9/.

4 Porosity measurement

Due to the specially chosen test signals $x_1(t)$ and $x_2(t)$ the function $\Phi_{xy1}(\tau)$ begins in the origin of coordinates and ends on the X axis when $\tau = t_{meas}$ (Fig. 5).

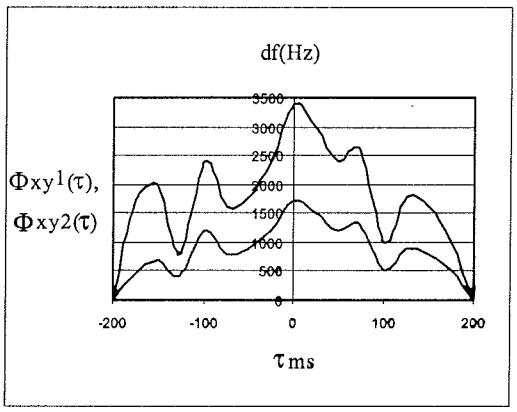

Fig. 5. Functions $\Phi_{xy1}(\tau)$ and $\Phi_{xy2}(\tau)$.

Consequently, the porosity is defined as a change of area between the functions $\Phi_{xy2}(\tau)$ and $\Phi_{xy1}(\tau)$, whose change is defined by capacitance C_x and specially chosen test signals $x_1(t)$ and $x_2(t)$. In this way the test signal has been considered throughout the entire t_{meas} period, as well as the sign change compensation in the calculation of the cross-correlation function. Comparing to the measurements that are not DDM method based the improvement of the ratio signal/noise by ≅ 30 dB is the most significant gain.

4.1 Calibration

The frequency is simultaneously converted into volume units by calibrating the ratio between the frequency and the volume for each glass tube. Mercury, whose mass is measured at an error of 0.01 % (at known temperature) is used for calibration /19/. The mechanical nonlinearities of the glass tube diameter along the whole tube are taken into account. According to the producer's data these do not exceed 0.01 %. The dependence can be linearized by using the spline method.

4.2 The influence of temperature and measurement error

The influence of temperature on measurements is considered in three ways. We must know the influence of the temperature on the measuring equipment, on the measuring medium in which the measurement is performed (i.e. the fluid in which the test is carried out), and the influence of the soil's temperature on its physical properties /19/.

The temperature of the environment affects the linearity of the measuring sensor. Calibration is used to establish the measurement error of the sensor which is 0.03 %. If the relation between the output frequency and the volume is known (Fig. 4), we get

$$V(T) = V(T_0) + \Delta V(T). \tag{30}$$

Equation (30) gives the correction of the measurement with respect to temperature changes. Temperature changes also affect the volume of the measured medium, i.e. of the

soil sample. Consequently, the change of volume due to temperature changes is expressed in the determination of the soil's specific gravity as follows

$$\gamma(T)=\gamma(T_0)+\Delta\gamma(T). \tag{31}$$

In conditions of linear temperature relationship inside a certain temperature range it holds true that

$$V(T)=V_s(T_0)\cdot\left(1+\alpha_{V_s}(T-T_0)\right) \tag{32}$$

where α_S is the temperature coefficient of soil.

The change of volume due to temperature changes in naturally humid soils is expressed as the sum of volume changes of all soil phases

$$dV(T)=dV_s(T)+dV_w(T)+dV_{ad}(T). \tag{33}$$

The total measurement error of the porosity sensor in relation to known individual partial influences such as glass tube nonlinearity, calibration with mercury, the influence of temperature on the sensor (Fig. 4), linearization of *df* on *V*, frequency measurement *y(t)* (Fig. 2), specific soil weight (31), change of water volume in the test tube and the change of sample volume *dV(T)* (33) does not exceed 0.1 % (10 - 30°C). This value was calculated on the basis of calibration data and the influence of temperature and measurement error.

5 Experimental porosity measurement

To test the new method, volcanic rock samples, which are known for their porosity, were selected for experimental determination of porosity. Four characteristic samples approximately 1 ml in size and 1 g in weight were gathered near Puerto de Santiago, Mount Teide volcano (3715 m), Tenerife (Fig. 6).

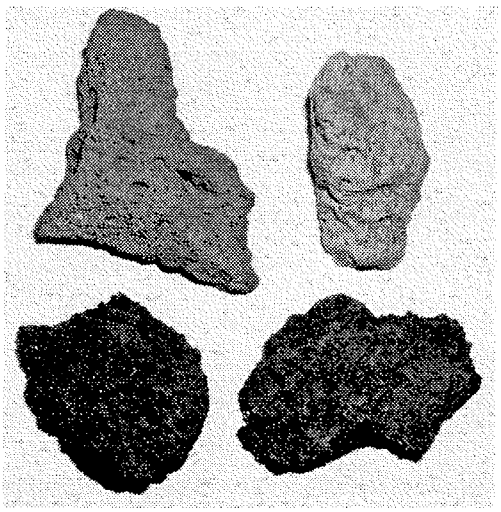

Fig. 6. Four typical porous volcanic rock samples of about 1 ml in size and 1 g in mass.

All test samples were randomly selected. To determine the porosity of a random solid sample (at 20 °C), the sample is immersed in water contained in a test tube around which the capacitor C_x is placed (Fig. 3). The volume of the sample is measured. In the first case, the glass solid sample with ~ 0 % porosity was immersed (Fig. 7).

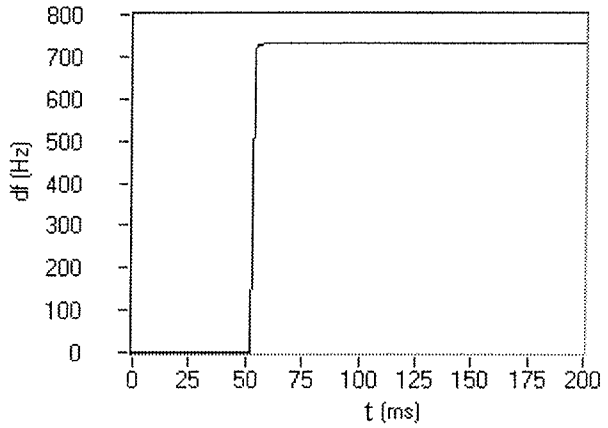

Fig. 7. Measurement of sample having ~ 0 % porosity.

The frequency remained unchanged after immersion, which indicates that there was no air leak. In the second case, a dry randomly selected volcanic rock sample (weighting 0.821 g) was immersed in the water. Since the sample was porous, the air leaked, which was reflected in the dynamic change of frequency (Fig. 8). The transitional phenomenon caused by immersion ends in 1 ms.

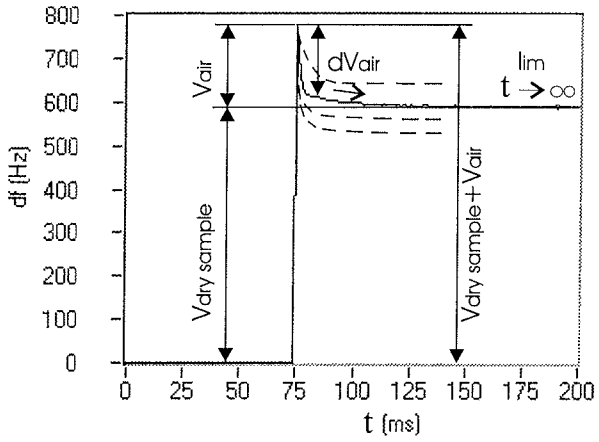

Fig. 8. Air leak after sample immersion.

The measurement is performed until the final state towards which the measurement limits is reliably predicted. Depending on the degree of porosity, this saturation limit is higher or lower as shown for the other three samples (Fig. 8).

At known temperature the sample porosity can be determined

$$\eta=\frac{V_{air}}{V_{drysample}+V_{air}}. \tag{34}$$

The sample porosity on Fig. 8 was 23.8 %. The fastest measurement time without test signals is 1 μs.

6 Conclusion

The porosity sensor using the capacitive-dependent crystals has been described and the dependence of *df* on the volume of the sensor probe has been presented. The porosity determination procedure includes the influence of test signals on the weighting function uncertainty.

The formation of the cross-correlation function between the test signal *x(t)* and the system response *y(t)* decreases the influence of all disturbing signals that are not correlated to the test signal x(t) for ≅ 30 dB /9/. Other advantages of the proposed method are high sensitivity, high stability, a series resonant circuit which is not composed of the elements *L* and *C*, the ratio signal/noise does not affect the accuracy of measurements, reduced disturbances due to the structure and the method, the long-term repetition, reduced hysteresis /17/ and low cost. It should be noted, however, that pairs of crystals with similar temperature characteristics should be used. The accuracy and repeatability are determined only with the temperature frequency difference of the crystal pairs /19/.

7 References

/1/ P. Sheng, „Effective medium theory of sedimentary rocks," Phys. Rev. B., vol. 41, pp. 4507, 1993.

/2/ S. Sakai, "Determination of pore size and pore size distribution," Journal of membrane science, vol. 96, pp. 91, 1994.

/3/ K. Meyer, P. Lorenz, B. Böhl-Kuhn, and P. Klobes, "Porous solids and their characterization," Cryst. Res. Techn., vol. 29, pp. 903, 1994.

/4/ A. Netto, "Pore-size distribution in sandstones," Bull. Appl. Math., vol. 77, pp. 1101, 1993.

/5/ J. Fredrich, B. Menendez, and T. Wong, "Imaging the pore structure of geomaterials," Science, vol. 268, pp. 276, 1995.

/6/ H. Franz, "Herstellung von Drucksensoren," Feinwerktechnik & Meâtechnik 95, H. 3, pp. 145-151, 1987.

/7/ J. Fripiat, „Porosity and adsorption isotherms," Fractal Approach to Heterogeneous Chemistry, Wiley, pp. 28, 1989.

/8/ G. P. P. Gunarathne and K. Christidis, "Measurements of Surface Texture Using Ultrasound," IEEE Trans. Instrum. Meas., 50 (5), October , pp. 1144-1148, 2002.

/9/ K. W. Bonfig, "Das Direkte Digitale Messverfahren (DDM) als Grundlage einfacher und dennoch genauer und störsicherer Sensoren," Sensor Nov., pp. 223-228, 1988.

/10/ M. C. McGregor, J. F. Hersh, R. D. Cutkosky, F. K. Harris, and F.R.Kotter, "New Apparatus at the National Bureau of Standards for Absolute Capacitance Measurement," IRE Trans. Instr. 1-7 (3-4), pp. 253-61, 1958.

/11/ A. M. Thompson, "The Precise Measurement of Small Capacitances," IRE Trans. Instr. 1-7(3-4), pp. 245-53, 1958.

/12/ G. L. Miller and E. R. Wagner, "Resonant phase shift technique for the measurement of small changes in grounded capacitors," Rev. Sci. Instrum. 61(4), pp.1267, 1990.

/13/ C. T. Van Degrift, "Modeling of tunnel diode oscillators," Rev. Sci .Instrum. 52(5), May, pp. 712-723, 1981.

/14/ K. Dmowski, "A new correlation method for improvement in selectivity of bulk trap measurements from capacitance and voltage transients," Rev. Sci. Instrum. 61(4), April, pp.1319-1325, 1990.

/15/ M. Bertocco, A. Flammini, D. Marioli, and A. Taroni, "Fast and Robust Estimation of Resonant Sensors Signal Frequency," IEEE Trans. Instrum. Meas., 51 (2), April, pp. 326-330, 2002.

/16/ V. Matko and J. Koprivnikar - a, "Capacitive sensor for water absorption measurement in glass-fiber resins using quartz crystals," IAAMSAD:South African branch of the Academy of Nonlinear Sciences, Proceedings, Durban, South Africa, pp. 440 -443, 1998.

/17/ V. Matko and J. Koprivnikar - b, "Quartz sensor for water absorption measurement in glass-fiber resins," IEEE Trans. Instrum. Meas., 47 (5), Oct., pp. 1159-1162, 1998.

/18/ M. Stucchi and K. Maex, "Frequency Dependence in Interline Capacitance Measurements," IEEE Trans. Instrum. Meas., 51 (3), Jun., pp. 537-543, 2002.

/19/ R. C. Weast, "CRC Handbook of Chemistry and Physic," 67 th edition, Boca Raton, Florida, pp. E49-E52, 1987.

Izr. prof. dr. Vojko Matko
University of Maribor, Faculty of Electrical Engineering and Computer Science,
Smetanova 17, 2000 Maribor, Slovenia
E-mail: vojko.matko@uni-mb.si

Prispelo (Arrived): 11.11.2002 *Sprejeto (Accepted): 25.05.2003*